

Centriole assembly in *Caenorhabditis elegans*

Laurence Pelletier¹, Eileen O'Toole², Anne Schwager¹, Anthony A. Hyman¹ & Thomas Müller-Reichert¹

Centrioles are necessary for flagella and cilia formation^{1,2}, cytokinesis^{3,4}, cell-cycle control⁵ and centrosome organization/spindle assembly⁶. They duplicate once per cell cycle, but the mechanisms underlying their duplication remain unclear. Here we show using electron tomography of staged *C. elegans* one-cell embryos that daughter centriole assembly begins with the formation and elongation of a central tube followed by the peripheral assembly of nine singlet microtubules. Tube formation and elongation is dependent on the SAS-5 and SAS-6 proteins, whereas the assembly of singlet microtubules onto the central tube depends on SAS-4. We further show that centriole assembly is triggered by an upstream signal mediated by SPD-2 and ZYG-1. These results define a structural pathway for the assembly of a daughter centriole and should have general relevance for future studies on centriole assembly in other organisms.

The structure of centrioles is conserved from ancient eukaryotes to mammals^{1,7–9}. They are barrel-shaped, 100–250 nm in diameter and 100–400 nm in length, with a ninefold symmetric array of singlet, doublet or triplet microtubules. Daughter centrioles grow orthogonally to the older (mother) centrioles, but the assembly process remains mysterious. Centrioles in *C. elegans* are 150 nm in length, 100 nm in diameter and consist of a central tube surrounded by nine singlet microtubules¹⁰. Genomic and genetic analyses have identified proteins required for centriole duplication in *C. elegans*^{11–16}. These include the ZYG-1 kinase, the SAS proteins (SAS-4, SAS-5 and SAS-6) and SPD-2, all of which localize to centrioles^{14,16–23}.

C. elegans oocytes arrest in meiotic prophase I, at which point they lack centrioles. Fertilization of oocytes by sperm triggers the completion of meiosis and contributes a centriole pair (Supplementary Fig. 1). After meiosis, the embryo enters the first mitotic division, which is characterized by a series of easily distinguishable events. These include pronuclear appearance (PNA), pronuclear migration (PNM), pronuclear rotation (PNR) and metaphase. Using chemical fixation and serial section electron microscopy we were able to detect daughter centriole assembly intermediates at, but not before, PNM (Supplementary Fig. 1).

To determine whether the onset of daughter centriole assembly correlates with the recruitment of known centriole proteins, we performed mating-based assays^{18,20,22–24} (Supplementary Fig. 2). In these assays, the sperm donates an unlabelled centriole pair, whereas the green fluorescent protein (GFP)-tagged centriole proteins are contributed by the maternal cytoplasm. Their incorporation into nascent daughter centrioles can therefore be monitored (Supplementary Fig. 2). We fixed embryos at different stages of the first cell division and stained them using SAS-4 antibodies—to mark the position of the sperm centrioles—and GFP or ZYG-1 antibodies to monitor the recruitment of individual centriole proteins to the site of assembly (Fig. 1; Supplementary Fig. 3 for GFP–ZYG-1 recruitment; $n > 10$ for each protein). We observed that SPD-2 and ZYG-1 are recruited to centrioles soon after fertilization, during the completion of female meiosis (Fig. 1a), whereas SAS-4, SAS-5 and SAS-6 are recruited shortly afterwards, at PNA (Fig. 1b).

To gain insights into the assembly relationship between these proteins, we depleted individual centriole proteins by RNA-mediated interference (RNAi) and determined the effect this had on the recruitment of the other proteins. In one-cell *spd-2(RNAi)* embryos ($n = 18$), we were unable to detect ZYG-1 recruitment at any stage (Fig. 2a, top panel); however, in *zyg-1(RNAi)* embryos, SPD-2 recruitment was unaffected ($n = 14$; Fig. 2a, bottom panel). These results suggest that SPD-2 acts upstream of ZYG-1. In all *spd-2(RNAi)* embryos analysed, we were unable to detect significant recruitment of maternal SAS-4, SAS-5 or SAS-6 to the site of centriole assembly (Fig. 2b, $n > 10$ for each protein). We observed essentially the same result in *zyg-1(RNAi)* embryos (data not shown), which is in agreement with previous results^{22–24} and with our observation that SPD-2 is required to recruit ZYG-1 (Fig. 2a). In *sas-4(RNAi)* embryos, both SAS-5 and SAS-6 are recruited to the site of daughter centriole assembly, confirming published results in two-cell embryos (Fig. 2c, $n = 4$)^{22,24}. It was previously shown that SAS-4 recruitment is blocked in *sas-5(RNAi)* and *sas-6(RNAi)* embryos^{22–24}. Together, these results suggest that in one-cell embryos SPD-2 and ZYG-1 are required for daughter centriole assembly by promoting the recruitment of the centriole components SAS-5 and SAS-6 (ref. 22). SAS-5 and SAS-6 recruitment then promotes the recruitment of SAS-4.

Our thin section electron microscopy results showed that daughter centriole assembly begins during PNM (Supplementary Fig. 1). In contrast, our mating assays showed that centriole proteins are recruited beforehand, during meiosis or at PNA (Fig. 1). Two possibilities could explain these observations. First, centriole proteins may be recruited to the proximity of the mother centrioles before daughter centriole assembly. Second, the recruitment observed may coincide with the emergence of a structural intermediate that is undetectable using chemical fixation and thin section electron microscopy (Supplementary Fig. 1). To examine potential structural intermediates of centriole assembly, we developed an approach to perform high-pressure freezing and electron tomography on isolated embryos at different stages of the first cell division (for measurements see Supplementary Fig. 4 and Supplementary Table 1)²⁵. To our surprise, daughter centriole assembly intermediates were observed at PNA (Fig. 3a). The smallest structure detected was a cylindrical tube approximately 60 nm in length, similar to the central tube of mother centrioles (Fig. 3a). Electron-dense appendages emanated from the singlet microtubules of mother centrioles (Fig. 3a, bottom left panel, arrowheads). During PNM, the central tubes of daughter centrioles were longer, reaching about 110 nm at the end of PNM (Fig. 3b and Supplementary Fig. 5). We observed that the central tube of daughter centrioles increased in diameter during PNM, whereas that of the mother centriole did not (Supplementary Fig. 5); this increase coincided with the appearance of an inner/outer wall structure on daughter centriole central tubes (Fig. 3c, right panel). Singlet microtubules began assembling around the central tube during PNR and by the end of PNR nine singlet microtubules were

¹Max Planck Institute of Molecular Cell Biology and Genetics, Pfotenhauerstrasse 108, 01307 Dresden, Germany. ²Boulder Laboratory for 3D Electron Microscopy of Cells, Department of Molecular, Cellular and Developmental Biology, Campus Box 347, University of Colorado, Boulder, Colorado 80309, USA.

observed (Fig. 3c). We detected hook-like appendages along the length of daughter central tubes at positions where singlet microtubules had yet to assemble (Fig. 3c, arrowheads, and data not shown). Singlet microtubule assembly did not seem to occur preferentially at distal or proximal extremities, although a slight positional bias for the

distal region of the central tube was observed (Supplementary Fig. 5). In summary, our tomography results show that in one-cell embryos, daughter centriole assembly begins with the formation of the central tube, which elongates and increases in diameter before the assembly of the nine singlet microtubules.

We looked at the effect of individually depleting centriole proteins on daughter centriole assembly. In *zyg-1(RNAi)* embryos, no daughter centriole structures were detected (Fig. 4a), consistent with the idea that in *zyg-1(RNAi)* embryos, the SAS-proteins are not recruited to the site of centriole assembly (Fig. 3b)^{22–24}. Similarly, in *sas-5(RNAi)* and *sas-6(RNAi)* embryos, no daughter centriole structures were observed (Supplementary Movie ‘SAS5RNAi’ and Fig. 4b, respectively). Most interestingly, in *sas-4(RNAi)* embryos at PNA central tubes of daughter centrioles still formed (Fig. 4c). After PNR, daughter centriole central tubes were longer (Supplementary Movie ‘SAS4RNAi’ and Supplementary Table 1), suggesting that tube elongation can still occur in *sas-4(RNAi)* embryos. Daughter centriole central tubes failed to increase in width, and seemed defective in the assembly of both singlet microtubules and hook-like appendages (Supplementary Table 1 and data not shown). In older embryos, daughter centriole central tubes were often difficult to discern (data not shown). These results are consistent with our observation for wild-type embryos that the formation of a central tube represents a structural intermediate in centriole assembly, which is unstable in *sas-4(RNAi)* embryos. Taken together, our electron tomography and light microscopy data suggest that SAS-4 is required to assemble or maintain singlet microtubules onto the central tube, the assembly of which is, in turn, dependent on SAS-5 and SAS-6.

Using electron tomography we have shown that daughter centriole assembly in one-cell *C. elegans* embryos occurs in at least three distinct steps: tube formation; tube elongation; and singlet microtubule assembly (Fig. 4d). Assembly begins at the time of PNA and is completed by the end of PNR, which we estimate requires 8–10 min (Fig. 4d). The recruitment of the SAS-proteins at PNA to the site of daughter centriole assembly is coincident with the emergence of the daughter central tube. In *spd-2(RNAi)* and *zyg-1(RNAi)* embryos, the recruitment of the SAS-proteins to the site of assembly is blocked. Accordingly, we were unable to detect daughter centriole structures in *zyg-1(RNAi)* embryos, confirming previous results¹⁴. These observations, in combination with our result showing that SPD-2 is required for the recruitment of the ZYG-1 kinase to the site of daughter centriole assembly, suggest that the role of SPD-2 in centriole duplication is to recruit ZYG-1 to centrioles (Fig. 4d). ZYG-1—possibly in concert with SPD-2—can then either function as a signal required for the initiation of daughter centriole assembly or directly drive the assembly process.

The fact that daughter centriole central tubes assemble in *sas-4(RNAi)* embryos (conditions under which SAS-5 and SAS-6 recruitment is not inhibited) indicates that SAS-5 and SAS-6 could be structural components of the central tube. SAS-5 and SAS-6 are known to physically interact, indicating that they may fulfil this structural role as a heterodimer²⁴. Alternatively, it is possible that SAS-5 and SAS-6 are required to maintain the structural integrity of the central tube, which is composed of other proteins. In

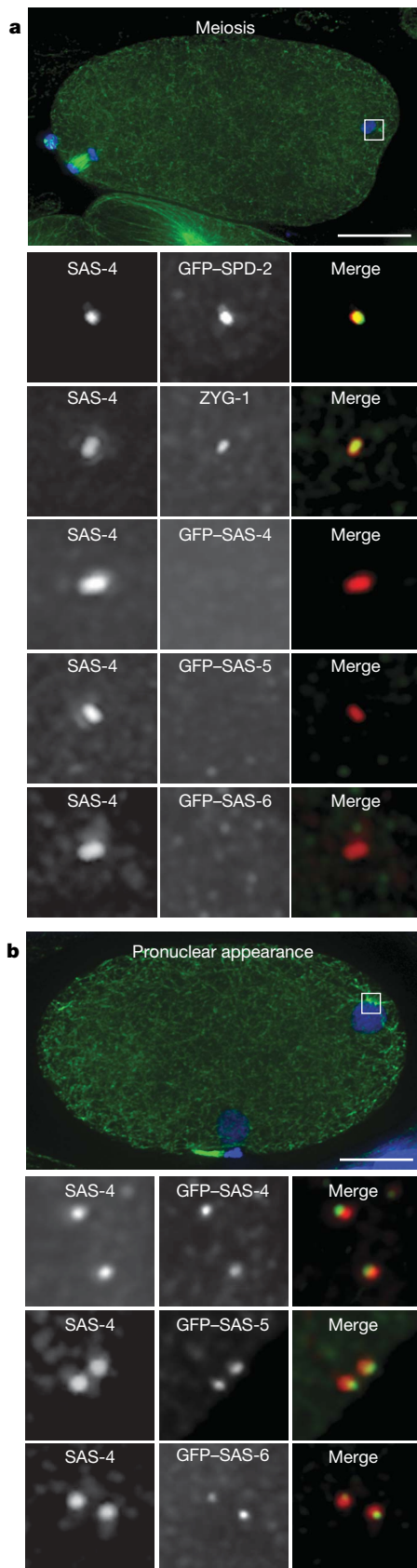


Figure 1 | Centriole proteins are recruited in two steps. **a**, Recruitment of centriole proteins during meiosis. At this stage only SPD-2 and ZYG-1 are recruited to centrioles, colocalizing with SAS-4. **b**, The SAS-proteins are recruited later, at the time of PNA. In these assays, wild-type males are mated to feminized hermaphrodites that express individual GFP-tagged centriole proteins. SAS-4 antibodies are used to label the sperm-derived centriole, therefore marking the site of daughter centriole assembly and GFP or ZYG-1 antibodies are used to monitor the recruitment of the maternal proteins. DNA (blue), microtubules (green), SAS-4 (white; red in merge) and GFP/ZYG-1 (white; green in merge) labels are shown. Given that ZYG-1 is not expressed in the sperm we used ZYG-1 antibodies to monitor the recruitment of the endogenous protein. Scale bars, 10 μ m.

sas-4(RNAi) embryos, central tube assembly is not perturbed although its stability and capacity to assemble singlet microtubules are compromised. Thus, we propose a role for SAS-4 in tethering singlet microtubules to the central tube, which would be consistent with the ring-like distribution of SAS-4 around centrioles²⁰. It was previously shown that the amount of SAS-4 on centrioles is related to the quantity of pericentriolar material they recruit²⁰. It is therefore possible that the singlet microtubules on the *C. elegans* centriole are required to recruit and organize pericentriolar material¹⁹. Recent evidence has shown that pericentriolar material is also required for daughter centriole assembly²³. It will be of interest to delineate the contribution of such proteins to daughter centriole assembly.

Published structures using chemical fixation and thin section electron microscopy on mammalian tissue culture cells are ambiguous as to whether centrioles have a central tube^{9,26,27}. It will be of importance to revisit daughter centriole assembly in mammalian tissue culture

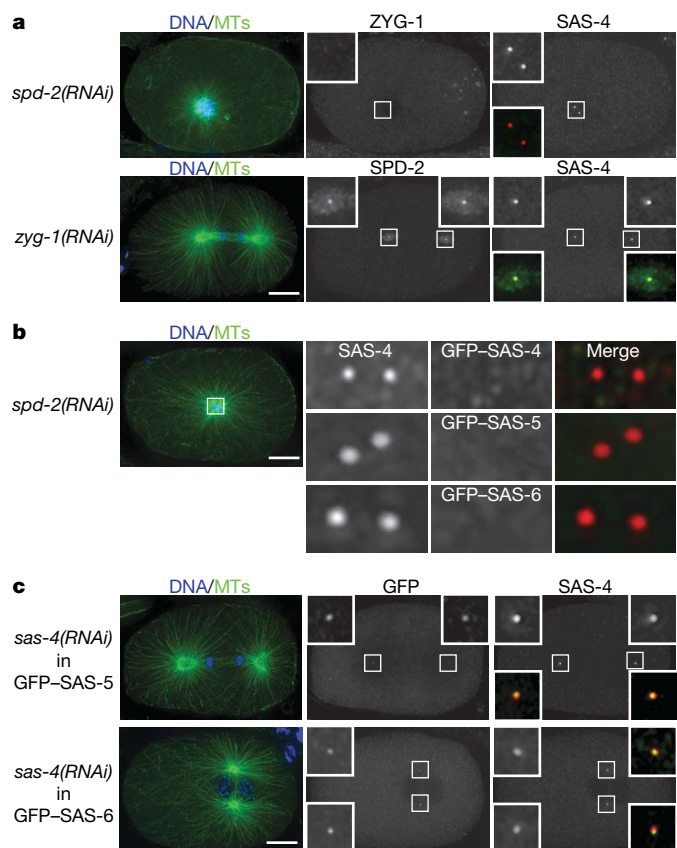


Figure 2 | SPD-2 and ZYG-1 are required for the recruitment of SAS proteins to the site of centriole assembly. **a–c**, The recruitment of individual centriole proteins was analysed in *spd-2(RNAi)*, *zyg-1(RNAi)* or *sas-4(RNAi)* embryos. **a**, In *spd-2(RNAi)* embryos ZYG-1 recruitment to centrioles is blocked (top panels). A merged image of ZYG-1 (green) with SAS-4 (red) is shown in the lower inset. In *zyg-1(RNAi)* embryos recruitment of SPD-2 is not affected (bottom panels). Merged images of SPD-2 (green) with SAS-4 (red) are shown in the lower insets. Insets are $\times 3$ magnification. **b**, In *spd-2(RNAi)* embryos, the recruitment of SAS-4, SAS-5 and SAS-6 to the site of daughter centriole assembly is blocked. Left panel shows the merged image of DNA (blue) and microtubules (green) of a representative *spd-2(RNAi)* embryo. Right panels show magnified ($\times 8$) views of SAS-4 immunolocalization; GFP-SAS-4, GFP-SAS-5 and GFP-SAS-6 labelling; and the respective merged images of regions similar to the boxed region shown in the merged image on the right. **c**, In *sas-4(RNAi)* embryos, recruitment of SAS-5 (top panel) and SAS-6 (bottom panel) still occurs. Merged images of GFP-SAS-5 (green) with SAS-4 (red) and of GFP-SAS-6 (green) with SAS-4 (red) are shown. Insets are $\times 3$ magnification. DNA (blue), microtubules (green), SAS-4 (white; red in merge) and GFP/ZYG-1/SPD-2 (white; green in merge) labels are shown. Scale bars, 10 μm .

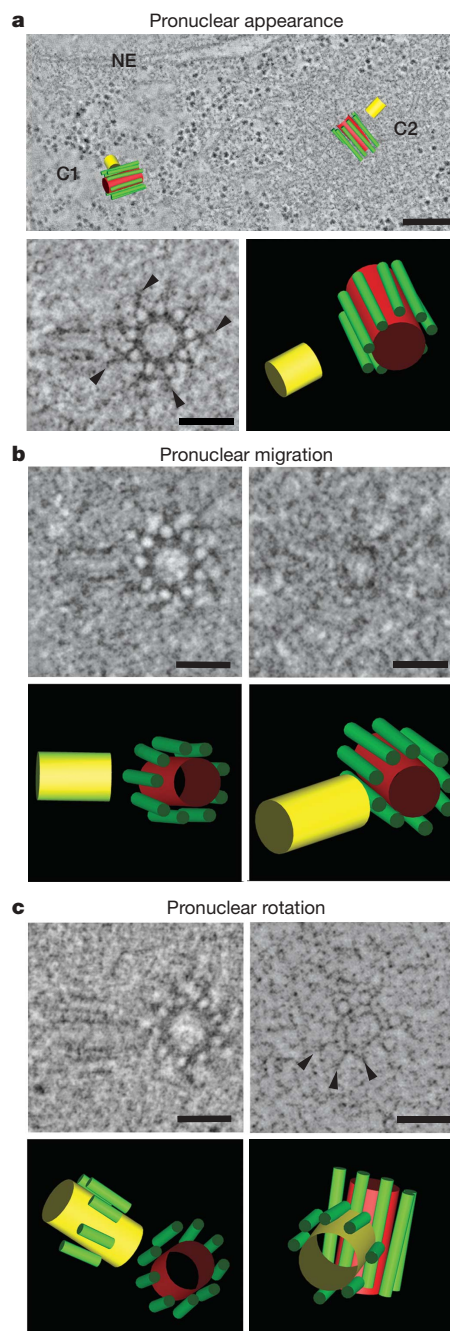


Figure 3 | Centriole assembly in *Caenorhabditis elegans* is a multi-step process. **a**, Tomographic slice and overlaid 3D model showing two centriole pairs (C1 and C2) at PNA (top). NE, nuclear envelope. Higher magnification view of another centriole pair at PNA (bottom left). The mother centriole is shown in cross-section and the assembling daughter centriole in longitudinal orientation. Note the presence of electron-dense appendages extending from the singlet microtubules of the mother centriole (arrowheads). Three-dimensional models illustrating the mother (red) and daughter (yellow) centriole central tubes and associated singlet microtubules (green) are also shown. **b**, Centrioles during PNM. The elongating central tubes of daughter centrioles are shown in both longitudinal orientation (left) and in cross section (right). **c**, Centrioles during PNR. An incomplete number of singlet microtubules are observed at this stage. Positions on the tube lacking singlet microtubules, but decorated with hook-like appendages, are indicated (arrowheads). Quicktime movies of all tomograms and 3D models can be found in Supplementary Information. Scale bars, 1 μm (top panel in **a**) and 100 nm (bottom panel in **a**, **b**, **c**).

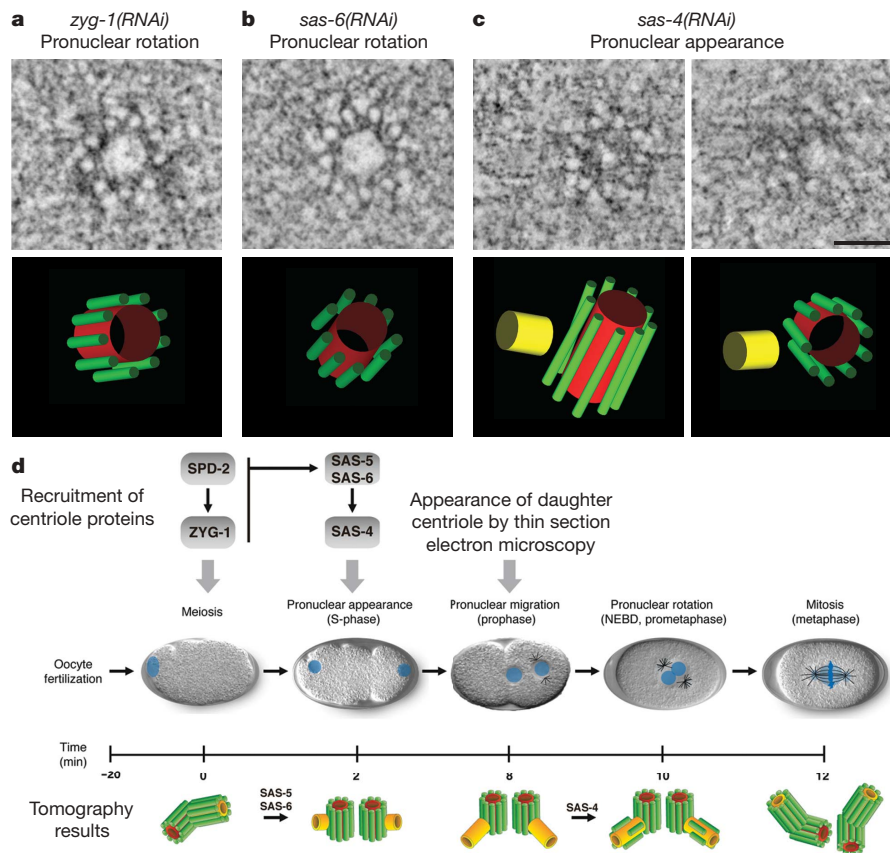


Figure 4 | The SAS proteins are required at different steps during centriole assembly. **a–c**, Tomographic reconstruction of *zyg-1(RNAi)* embryos during PNR (**a**), *sas-6(RNAi)* embryos during PNR (**b**), and *sas-4(RNAi)* embryos at PNA (**c**). Note the absence of daughter centriole structures in both *zyg-1(RNAi)* and *sas-6(RNAi)* embryos; but the presence of a daughter centriole central tube in *sas-4(RNAi)* embryos. Three-dimensional models illustrating the mother (red) and daughter (yellow) centriole central tubes and associated singlet microtubules (green) are shown in the bottom panels. Quicktime movies of all tomograms and 3D models can be found in Supplementary Information. **d**, Schematic representation of daughter centriole assembly during the first mitotic division. SPD-2 and ZYG-1 are

recruited during meiosis, before daughter centriole assembly. SPD-2 is required to recruit ZYG-1 to mother centrioles. Both SPD-2 and ZYG-1 are required for the recruitment of the SAS proteins at the time of PNA, coincident with the formation of the daughter centriole central tube. SAS-5 and SAS-6 are required for SAS-4 recruitment. In *sas-5(RNAi)* and *sas-6(RNAi)* embryos the central tubes fail to assemble. The central tube elongates during PNM and singlet microtubules assemble around it during PNR in a SAS-4 dependent fashion so that by metaphase two fully formed daughter centrioles are observed. NEBD, nuclear envelope breakdown. Scale bar, 100 nm.

cells, and other organisms, using high-pressure freezing and time-resolved tomography to determine if daughter centriole assembly also proceeds in the same order: tube formation, elongation and microtubule assembly. Interestingly, three of the five components required for centriole duplication in *C. elegans*—SPD-2, SAS-4 and SAS-6—have mammalian homologues^{17,18,23,24}, although only human SAS-6 is known to be required for centriole duplication. It is therefore likely that some of the assembly intermediates uncovered here in *C. elegans* are conserved in mammals and other eukaryotes.

Note added in proof: While this paper was being reviewed, another study²⁹ reported the sequential recruitment of *C. elegans* centriole proteins during duplication.

METHODS

***Caenorhabditis elegans* strains, RNAi and immunofluorescence.** The worm strains, antibodies, dsRNA and RNAi conditions used in this study are detailed in Supplementary Information. For immunofluorescence microscopy embryos were labelled and imaged as previously described¹⁷. Three-dimensional data sets were acquired on a DeltaVision RT imaging system (Applied Precision) and shown as maximal projections.

Specimen preparation for electron tomography. Hermaphrodites were dissected in M-9 buffer containing 20% BSA (weight by volume; Sigma), individual embryos collected into capillary tubing, and development observed using phase

contrast microscopy. Embryos at specific stages were transferred to specimen holders and frozen using the EMPACT2+RTS high-pressure freezer (Leica). Embryos were freeze-substituted, stained and imaged by electron tomography using a TECNAI F30 intermediate-voltage electron microscope (FEI) operated at 300 kV as previously described²⁵.

Modelling and analysis of tomographic data. We recorded five double-tilt data sets of poles at PNA, five at PNM, five during PNR and six during mitosis. In addition, we acquired two data sets of *zyg-1(RNAi)* embryos, four of *sas-4(RNAi)* embryos, two of *sas-5(RNAi)* embryos and three of *sas-6(RNAi)* embryos. Tomography and image analysis was carried out using the IMOD software package²⁸. Using serial slices extracted from the tomograms, we modelled the central tube and the singlet microtubules of mother and daughter centrioles. The structure of assembly intermediates was analysed by extracting a slice of image data 1-voxel thick. The orientation was adjusted to visualize the centriole in either longitudinal orientation or in cross-section. The projections of the 3D models were displayed and rotated to study their 3D geometry. To display in 3D, substructures of the centriole were meshed using the IMODMESH program and shown as tubular graphical objects. Measurements of centriole components were extracted from model contour data using the companion program, IMODINFO (Supplementary Fig. 6 and 7).

Received 25 August; accepted 6 October 2006.

1. Dutcher, S. K. Elucidation of basal body and centriole functions in *Chlamydomonas reinhardtii*. *Traffic* 4, 443–451 (2003).

2. Briggs, L. J., Davidge, J. A., Wickstead, B., Ginger, M. L. & Gull, K. More than one way to build a flagellum: comparative genomics of parasitic protozoa. *Curr. Biol.* **14**, R611–R612 (2004).
3. Gromley, A. *et al.* Centriolin anchoring of exocyst and SNARE complexes at the midbody is required for secretory-vesicle-mediated abscission. *Cell* **123**, 75–87 (2005).
4. Piel, M., Nordberg, J., Euteneuer, U. & Bornens, M. Centrosome-dependent exit of cytokinesis in animal cells. *Science* **291**, 1550–1553 (2001).
5. Doxsey, S., McCollum, D. & Theurkauf, W. Centrosomes in cellular regulation. *Annu. Rev. Cell Dev. Biol.* **21**, 411–434 (2005).
6. Sluder, G. & Rieder, C. L. Centriole number and the reproductive capacity of spindle poles. *J. Cell Biol.* **100**, 887–896 (1985).
7. Azimzadeh, J. & Bornens, M. in *Centrosomes in Development and Disease* (ed. Nigg, E. A.) 93–122 (Wiley-VCH, Weinheim, 2004).
8. Dippell, R. V. The development of basal bodies in paramecium. *Proc. Natl Acad. Sci. USA* **61**, 461–468 (1968).
9. Vorobjev, I. A. & Chentsov Yu, S. Centrioles in the cell cycle. I. Epithelial cells. *J. Cell Biol.* **93**, 938–949 (1982).
10. O'Toole, E. T. *et al.* Morphologically distinct microtubule ends in the mitotic centrosome of *Caenorhabditis elegans*. *J. Cell Biol.* **163**, 451–456 (2003).
11. Gönczy, P. *et al.* Functional genomic analysis of cell division in *C. elegans* using RNAi of genes on chromosome III. *Nature* **408**, 331–336 (2000).
12. Sönnichsen, B. *et al.* Full-genome RNAi profiling of early embryogenesis in *Caenorhabditis elegans*. *Nature* **434**, 462–469 (2005).
13. Zipperlen, P., Fraser, A. G., Kamath, R. S., Martinez-Campos, M. & Ahringer, J. Roles for 147 embryonic lethal genes on *C. elegans* chromosome I identified by RNA interference and video microscopy. *EMBO J.* **20**, 3984–3992 (2001).
14. O'Connell, K. F. *et al.* The *C. elegans zyg-1* gene encodes a regulator of centrosome duplication with distinct maternal and paternal roles in the embryo. *Cell* **105**, 547–558 (2001).
15. O'Connell, K. F., Leys, C. M. & White, J. G. A genetic screen for temperature-sensitive cell-division mutants of *Caenorhabditis elegans*. *Genetics* **149**, 1303–1321 (1998).
16. O'Connell, K. F., Maxwell, K. N. & White, J. G. The *spd-2* gene is required for polarization of the anteroposterior axis and formation of the sperm asters in the *Caenorhabditis elegans* zygote. *Dev. Biol.* **222**, 55–70 (2000).
17. Pelletier, L. *et al.* The *Caenorhabditis elegans* centrosomal protein SPD-2 is required for both pericentriolar material recruitment and centriole duplication. *Curr. Biol.* **14**, 863–873 (2004).
18. Leidel, S. & Gönczy, P. SAS-4 is essential for centrosome duplication in *C. elegans* and is recruited to daughter centrioles once per cell cycle. *Dev. Cell* **4**, 431–439 (2003).
19. Leidel, S. & Gönczy, P. Centrosome duplication and nematodes: recent insights from an old relationship. *Dev. Cell* **9**, 317–325 (2005).
20. Kirkham, M., Müller-Reichert, T., Oegema, K., Grill, S. & Hyman, A. A. SAS-4 is a *C. elegans* centriolar protein that controls centrosome size. *Cell* **112**, 575–587 (2003).
21. Kemp, C. A., Kopish, K. R., Zipperlen, P., Ahringer, J. & O'Connell, K. F. Centrosome maturation and duplication in *C. elegans* require the coiled-coil protein SPD-2. *Dev. Cell* **6**, 511–523 (2004).
22. Delattre, M. *et al.* Centriolar SAS-5 is required for centrosome duplication in *C. elegans*. *Nature Cell Biol.* **6**, 656–664 (2004).
23. Dammermann, A. *et al.* Centriole assembly requires both centriolar and pericentriolar material proteins. *Dev. Cell* **7**, 815–829 (2004).
24. Leidel, S., Delattre, M., Cerutti, L., Baumer, K. & Gönczy, P. SAS-6 defines a protein family required for centrosome duplication in *C. elegans* and in human cells. *Nature Cell Biol.* **7**, 115–125 (2005).
25. Müller-Reichert, T., Srayko, M., Hyman, A., O'Toole, E. & McDonald, K. Correlative light and electron microscopy of early *Caenorhabditis elegans* embryos in mitosis. *Meth. Cell Biol.* **79**, 99–117 (in the press).
26. Kuriyama, R. & Borisy, G. G. Centriole cycle in Chinese hamster ovary cells as determined by whole-mount electron microscopy. *J. Cell Biol.* **91**, 814–821 (1981).
27. Robbins, E., Jentsch, G. & Micali, A. The centriole cycle in synchronized HeLa cells. *J. Cell Biol.* **36**, 329–339 (1968).
28. Kremer, J. R., Mastronarde, D. N. & McIntosh, J. R. Computer visualization of three-dimensional image data using IMOD. *J. Struct. Biol.* **116**, 71–76 (1996).
29. Delattre, M., Canard, C. & Gönczy, P. Sequential protein recruitment of *C. elegans* centriole formation. *Curr. Biol.* **16**, 1844–1849 (2006).

Supplementary Information is linked to the online version of the paper at www.nature.com/nature.

Acknowledgements We thank A. Dammermann and K. Oegema for their gift of the GFP-ZYG-1 strain and for sharing unpublished results; F. Barr for anti-GFP antibodies; M. Tipsword, M. Ruer and D. Drechsel for generating the ZYG-1 antibodies; A. Pozniakovsky for generating the GFP-SAS-5 and GFP-SAS-6 constructs; O. Molodtsova for biolistic bombardment; J. Mäntler and Q. DeRobillard for help with electron microscopy; C. Lorenz for secretarial assistance; K. McDonald, P. Verkade and I. Baines for help in developing the single-embryo high-pressure freezing approach; C. Eckmann for providing the FOG-1 feeding construct; and F. Friedrich for help with graphical artwork. We are grateful to G. Warren, W. Zacheriae, R. Kittler and F. Quittnat Pelletier for their comments on the manuscript, and Hyman laboratory members for stimulating discussions. The Boulder Laboratory for 3D Electron Microscopy of Cells is supported by a grant from the National Institutes of Health to J. R. McIntosh. L.P. is supported by a postdoctoral fellowship from the HFSP.

Author Information Reprints and permissions information is available at www.nature.com/reprints. The authors declare no competing financial interests. Correspondence and requests for materials should be addressed to L.P. (pelletie@mpi-cbg.de).